Sedimentology (2004) **51,** 1145–1154 doi: 10.1111/j.1365-3091.2004.00665.x

Terrigenous sedimentation processes along the continental margin off NW Africa: implications from grain-size analysis of seabed sediments

CHRISTINE HOLZ, JAN–BEREND W. STUUT and RÜDIGER HENRICH
Department of Geosciences, University of Bremen, Klagenfurter Straße, 28359 Bremen, Germany (E-mail: cholz@uni-bremen.de)

ABSTRACT

The terrigenous fraction of seabed sediments recovered along the north-west African continental margin illustrates spatial variability in grain size attributed to different transport mechanisms. Three subpopulations are determined from the grain-size analyses ($n = 78$) of the carbonate-free silt fraction applying an end-member modelling algorithm (G. J. Weltje, 1997). The two coarsest end-members are interpreted as representing aeolian dust, and the fine-grained end-member is related to fluvial supply. The end-member model thus allows aeolian fallout to be distinguished from fluvial-sourced mud in this area. The relative contributions of the end-members show distinct regional variations that can be related to different transport processes and pathways. Understanding present-day sediment dispersal and mixing is important for a better understanding of older sedimentary records and palaeoclimate reconstructions in the region.

Keywords Aeolian dust, Canary Islands, carbonate-free silt, deep-sea sediments, end-member modelling, grain size, Sahara.

INTRODUCTION

Satellite images of large dust clouds over the North Atlantic Ocean (Fig. 1) indicate that the area off NW Africa occupies a key position with respect to the aeolian dust contribution from Saharan and Sahelian latitudes. At present, the Sahara–Sahel area is one of the most important global source regions of airborne mineral dust (Middleton *et al.*, 1986; Bergametti, 1992; Harrison *et al.*, 2001). The Sahara produces more aeolian dust than any other world desert, and this dust has an important impact on climatic processes, nutrient cycles, soil formation and sediment cycles (Goudie & Middleton, 2001). D'Almeida (1989) estimated the amount of Saharan dust at 0·6–0·7 pg ($= 10^{15}$) year^{-1}, of which about one-third is deposited in the North Atlantic Ocean (Duce *et al.*, 1991). The particle-size distribution of the transported dust depends, among other things, on the transport distance. Proximal aeolian dust particles may be up to 50 μm in diameter (D'Almeida & Schütz, 1983; Pye, 1987; Duce, 1995). Harmattan dust at Kano (Nigeria) can have a median diameter up to 74 μm (McTainsh & Walker, 1982), while samples taken over Sal Island (Cape Verde Islands) off west Africa yielded individual quartz grains up to 90 μm in diameter (Glaccum & Prospero, 1980). Conversely, aerosols reaching the Caribbean (Goudie & Middleton, 2001) may be less than 5 μm in size (Talbot *et al.*, 1986). However, the mean modal and median sizes of the transported aeolian dust were shown to be fine silt between 5 and 30 μm in diameter (Goudie & Middleton, 2001), and many soils in desert marginal areas appear to contain significant quantities of silt (McTainsh, 1987). As previous marine studies in regions downwind of major deserts have shown, mineral dust is a major component not only of the atmosphere but also of deep-sea sediments (Koopmann, 1981; Sarnthein *et al.*, 1982; Moreno *et al.*, 2002; Stuut *et al.*, 2002). However, terrigenous sedimentation along continental margins is also influenced by river discharge and hemipelagic settling (Koopmann, 1981; Sarnthein *et al.*, 1982; Sirocko *et al.*, 1991). To distinguish between different transport mechanisms for terrigenous sediments, a

© 2004 International Association of Sedimentologists

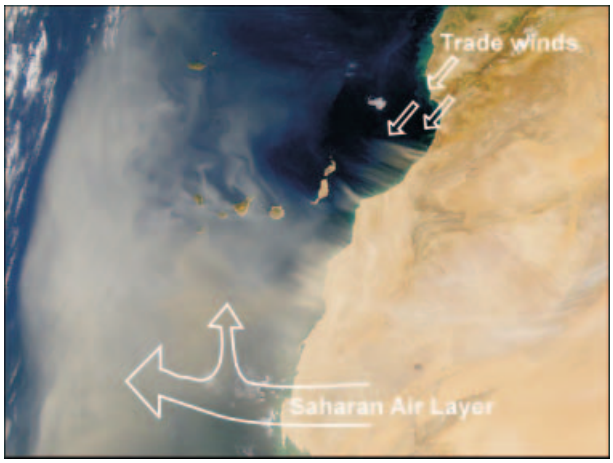

Fig. 1. Satellite image of a dust storm off north-west Africa, acquired in winter by the sea-viewing wide field-of-view sensor (SeaWiFS), NASA Goddard Space Flight Center, and ORBIMAGE. Arrows mark the present-day relevant wind systems: the Saharan Air Layer (SAL) and the NE trade winds.

numerical–statistical algorithm (Weltje, 1997) was applied to the carbonate-free grain-size distributions of the silt fraction of seabed samples offshore north-west Africa. The end-member algorithm attempts to explain observed variations in natural sediments as a result of mixing and has been used successfully to 'unmix' sediments produced by linear mixing (Prins & Weltje, 1999; Prins *et al.*, 2000, 2002; Moreno *et al.*, 2002; Stuut *et al.*, 2002; Arz *et al.*, 2003; Frenz *et al.*, 2003). The purpose of the present study is: (1) to describe the spatial variability in grain size of seabed samples along the continental slope adjacent to a major desert with emphasis on the carbonate-free silt fraction; and (2) to deduce transport pathways and mechanisms of land-derived sediments using the end-member modelling approach.

INVESTIGATION AREA

The investigated area along the continental margin of north-west Africa extends from the Moroccan coast at about 33°N to the Mauritanian coast off Nouakchott at about 17°N (Fig. 2). The continental shelf is generally narrow, between 40 and 60 km wide (Wynn *et al.*, 2000a), although maximum shelf widths between 100 and 120 km occur near stable massifs north and south of Cape Blanc (Seibold & Fütterer, 1982). Slope angles generally vary from 1 to 6° although, in some restricted areas, e.g. adjacent to the Western Sahara Canyon System, slope angles may reach 40° (Wynn *et al.*, 2000a). Seismic studies illustrate that large sections of the north-west African slope are dissected by canyon systems and channels. In addition, numerous volcanic islands provide a complex submarine topography (Weaver *et al.*, 2000; Wynn *et al.*, 2000a,b; Masson *et al.*, 2002).

The major surface current in this area is the Canary Current (Mittelstaedt, 1991), which is part of the Eastern Boundary Current System and is characterized by south-westward flow. Deep-water bottom currents on the north-west African margin are represented by south-flowing carbonate-saturated North Atlantic Deep Water (NADW) (at a depth of 2000–3800 m) and, below this, the north-flowing, carbonate-corrosive Antarctic Bottom Water (AABW). Bottom current velocities are thought to be fairly weak (< 5 cm s^{-1}) at present, whereas in areas where currents are focused by morphology or in areas with additional tidal components, velocities may increase to 20 cm s^{-1} (Lonsdale, 1982; Sarnthein *et al.*, 1982).

Lying adjacent to and downwind of the Saharan desert, the investigated area is directly connected to a large source of aeolian dust, and it lies beneath the prevailing dust-loaded wind trajectories. The most relevant wind systems are the Saharan Air Layer (SAL) and the north-east trade winds, the latter causing coastal upwelling off NW Africa. Owing to the meridional displacement of the Azores high-pressure system, the trade-wind belt and the Intertropical Convergence Zone (ITCZ) show a seasonal variability, and therefore the centre of transatlantic aeolian dust transport migrates seasonally. During the summer, the high-pressure system is situated in a northerly position with major trade wind activity between 32°N and 20°N. Conversely, during winter, the subtropical high-pressure centre shifts to the south, and trade winds blow most intensely between 25°N and 10°N. Thus, between 20°N and 25°N, trade winds and coastal upwelling are important throughout the year. The source regions for the SAL are the southern Sahara and the adjacent Sahel zone (Koopmann, 1981; Sarnthein *et al.*, 1982). This dust is transported westward. The SAL is divided into a northern branch, which disperses aeolian sediment over the north-east Atlantic Ocean and the Canary Islands, and a western branch that transports the aerosols far offshore (Fig. 1). Small particles may eventually reach the Caribbean and the SE United States (Prospero & Carlson, 1972).

There is another major source of terrigenous sediments apart from aeolian dust; in the northern part of the study area, a number of seasonal

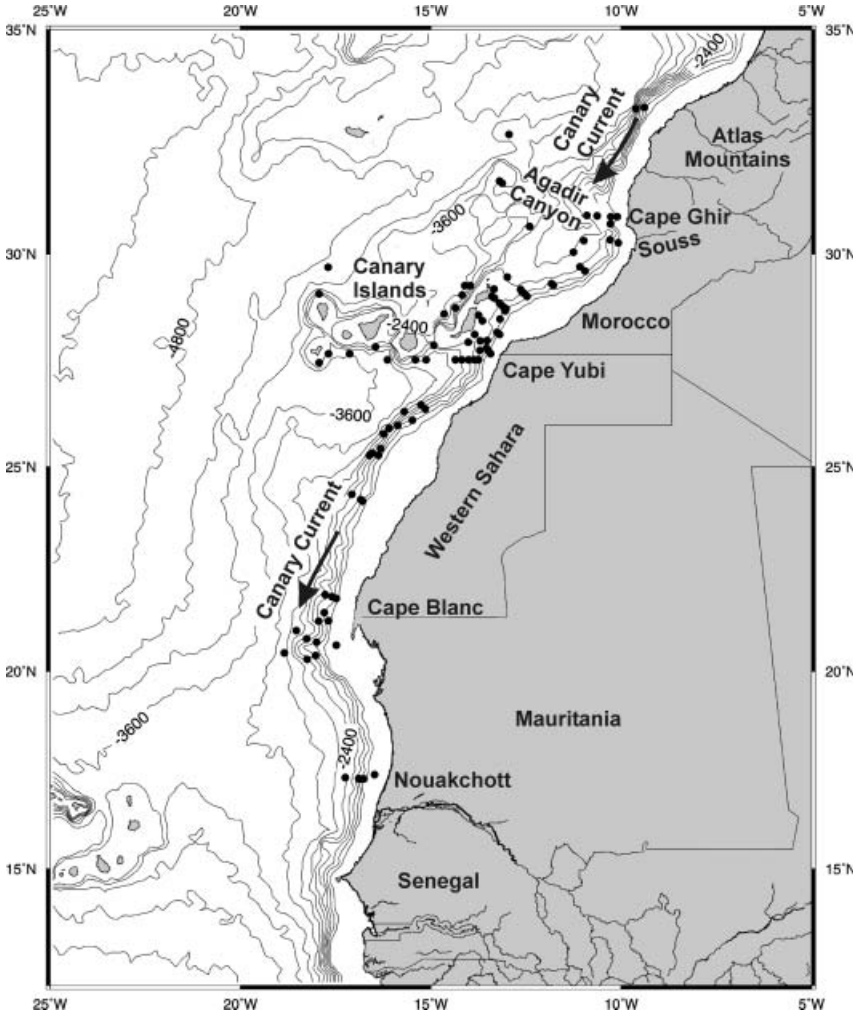

Fig. 2. Map of the north-west African continental margin showing seabed sample locations and the general pattern of surface currents. Map is generated with GMT (Wessel & Smith, 1991) using altimetry and ship depth sounding data from Smith & Sandwell (1997).

rivers transport sediment derived from the Atlas Mountain hinterland to the continental shelf (Wynn *et al.*, 2000a). The total sediment discharge of north-west African rivers is estimated to be 110 million tons year^{-1} (Milliman & Meade, 1983; Hillier, 1995). Today, the major proportion of these fluvial sediments is deposited on the continental shelf. However, numerous canyons, dissecting the shelf break, provide conduits through which the material may be bypassed to the Seine Abyssal Plain and the Agadir Basin and Madeira Plain (Weaver *et al.*, 2000; Wynn *et al.*, 2000a). The canyon systems in the northern part of the north-west African continent have been shown still to be influenced by fluvial drainage (Ercilla *et al.*, 1998; Wynn *et al.*, 2000a), whereas further to the south, on the western Saharan margin between 17° and 28°N, fluvial supply is significantly reduced compared with the area north of 29°N (Wynn *et al.*, 2000a). Here, rivers reach the Atlantic Ocean only seasonally and, along the majority of the margin, there is no significant fluvial input at all (Wynn *et al.*, 2000a).

MATERIALS AND METHODS

A total of 96 marine seabed samples (taken with a multicorer and a giant boxcorer within a depth range of 100–4200 m) was recovered in the Canary Island region between the years 1996 and 1999 during several cruises of the *RV Meteor*, *RV Poseidon* and *RV Victor Hensen* (Fig. 2). These samples from the uppermost centimetre of the sea floor were freeze-dried and, after removing the organic matter through oxidation with 10% H_2O_2, the fine fraction (< 63 μm) was separated by wet-sieving. The silt fraction (2–63 μm) was extracted from clay particles by a repeated settling procedure based on Stokes' law using Atterberg settling tubes. The relative proportions of the sand, silt and clay fractions were determined. In a first approach, the grain size of each bulk silt sample

was measured using a Micromeritics SediGraph 5100. This fine-particle size analyser determines particle sizes in the range of 0·1–300 μm (Coakley & Syvitski, 1991) and is a robust device for fine sediment (< 63 μm). Afterwards, the calcareous silt was dissolved with 1 N HCl and washed repeatedly until the pH was neutral. Then, the grain-size distribution of the carbonate-free silt fraction was analysed for 78 samples (18 samples contained too little material for a proper measurement). As the biogenic silica component is evanescent (Koopmann, 1981; Sarnthein *et al.*, 1982) and can be neglected, the carbonate-free silt fraction is considered as the clastic silt fraction. For a better interpretation of the grain-size data, a numerical–statistical algorithm (Weltje, 1994, 1997) was applied to model the grain-size distributions using the grain-size results of 78 carbonate-free silt samples. The end-member algorithm aims to describe the variance in the total data set with a number of subpopulations, so-called 'end-members'. Goodness-of-fit statistics provide the estimation of the minimum number of end-members by calculating the coefficient of determination (r^2) that is required for a satisfactory approximation of the data. R^2 represents the proportion of the variance of each grain-size class that can be reproduced by the approximated data. This proportion is equal to the squared correlation coefficient (r^2) of the input variables and their approximated values (Weltje, 1997; Prins & Weltje, 1999).

Present-day aeolian dust fallout was collected along a transect (33°N to 12°S) of the African west coast during *RV Meteor* cruise M41/1 (Schulz *et al.*, 1998) using an Anderson dust sampler model GMWL 2000, which was located ≈15 m above sea level. The dust was rinsed off the filter according to the method described by Kiefert (1994) and Kiefert *et al.* (1996) using demineralized water instead of trisodium orthophosphate (Stuut, 2001). The grain-size distributions of the aeolian dust were measured with a Coulter LS230 at NIOZ (Royal Netherlands Institute for Sea Research, Texel, The Netherlands), resulting in grain-size distributions ranging from 0·4 to 2000 μm (Fig. 3).

RESULTS

Grain-size distributions

The mean grain-size classification (sand/silt/clay) of seabed sediments off NW Africa is shown in

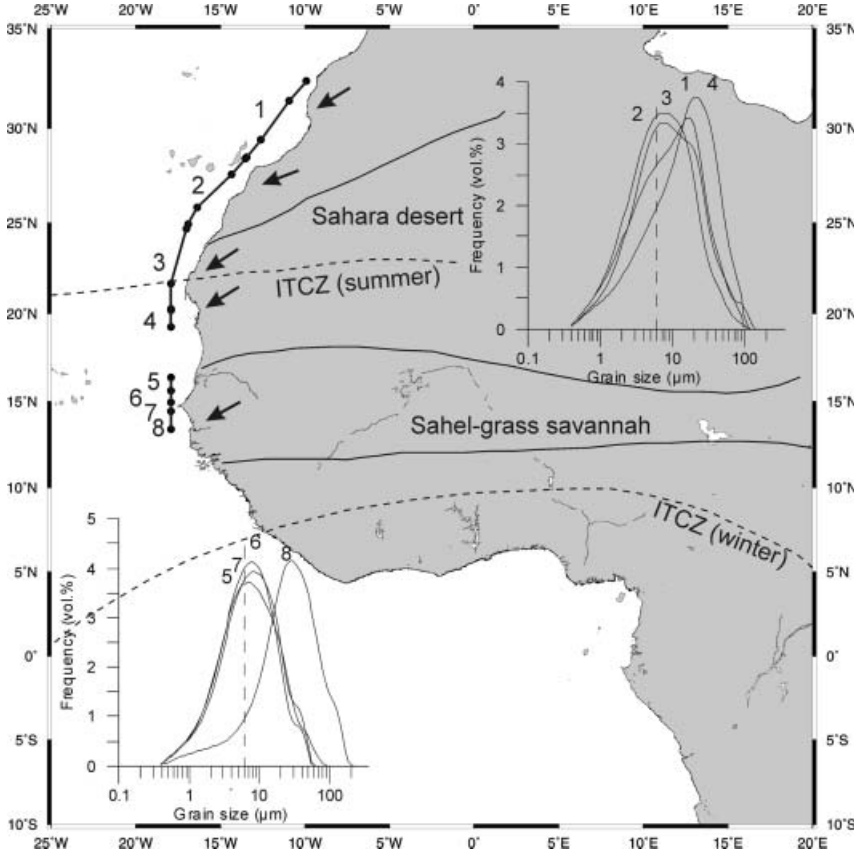

Fig. 3. Grain-size distributions of present-day aeolian dust collected off the west African coast with a dust sampler on board the *RV Meteor*. The grain-size distributions shown are the result of collecting dust fallout along the illustrated transects (black lines; black dots mark the beginning and end of each sampling period). Arrows illustrate prevailing true surface wind directions. The dotted lines indicate the summer and winter position of the Intertropical Convergence Zone (ITCZ). Relevant vegetation zones, the Sahara desert and the Sahel zone are shown.

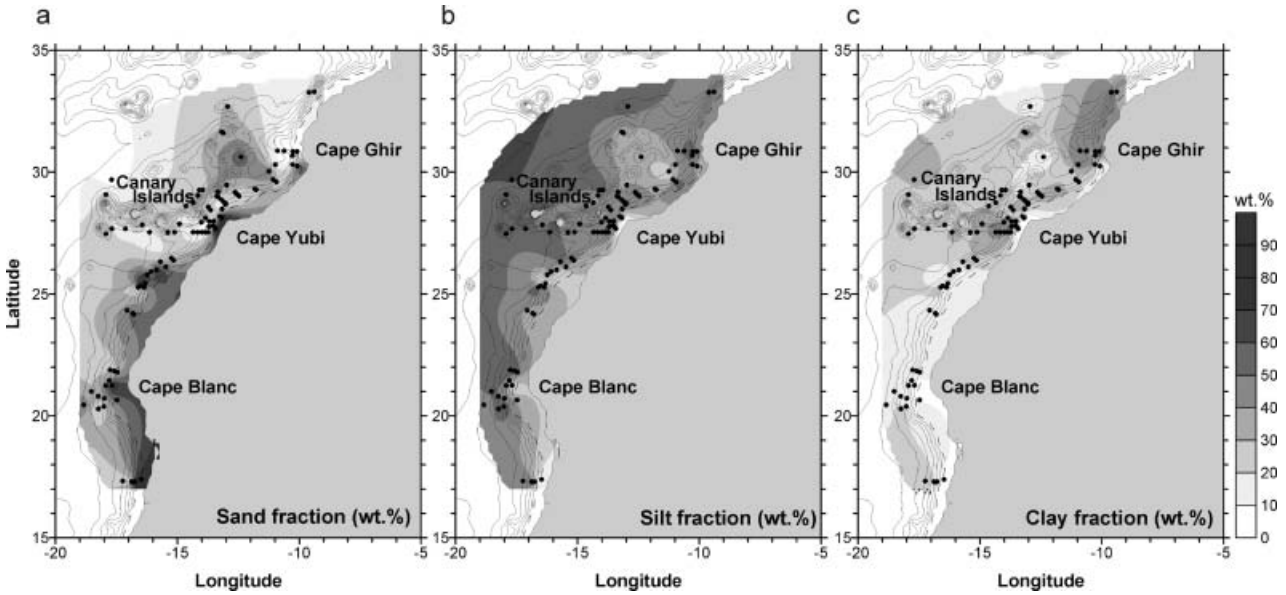

Fig. 4. Distribution maps of different grain-size classes (wt%) for seabed sediments along the north-west African continental margin. (a) Sand (> 63 μm), (b) silt fraction (63–2 μm) and (c) clay content (< 2 μm) in weight percentages. Isopleths were calculated using the gridding method of kriging. The dashed line displays the 200 m water-depth isoline and represents approximately the shelf break.

Fig. 4. Generally, the highest amounts of coarser sediment (e.g. sand and silt) are on the continental shelf while, with increasing distance from the shelf, the grain size decreases. The area off Cape Ghir is conspicuous with a relatively low proportion of sand and high clay contents up to 50 wt% (Fig. 4a and c).

End-member modelling results of the carbonate-free silt fraction

Polymodal grain-size distribution patterns of the carbonate-free silt fraction prevent any reliable interpretation of the grain-size moment statistics in terms of sediment transport mechanisms or sediment sources. To be able to interpret the observed grain-size data in terms of sediment transport mechanisms, end-members were calculated using grain-size distributions of 78 samples (Fig. 5). These end-members represent a series of fixed sediment grain-size compositions that can be regarded as subpopulations within the data set of seabed samples (Weltje, 1997). Figure 5a shows the mean size distribution and maximum range of frequency for each size class of all modelled samples ($n = 78$). In Fig. 5b, the coefficient of determination for each size class is shown for end-member models ranging from two to 10 end-members. The mean coefficients of determination (r^2) are plotted for several end-member models (Fig. 5c). In general, the mean coefficient of determination of the different end-member models increases with increasing numbers of end-members (Fig. 5c). The two-end-member model shows small values of coefficient of determination ($r^2 < 0{\cdot}6$) for the grain-size spectrum 12–24 μm; the three-end-member model ($r^2_{mean} = 0{\cdot}87$) reveals relatively low r^2 for the size range 15–20 μm only. Better statistical fit is gained with the four- to 10-end-member models. For the four-end-member model, the mean coefficient of determination ($r^2_{mean} = 0{\cdot}91$) increases only slightly relative to that of the three-end-member model. Hence, with regard to the contradictory requirements of parsimony on the one hand (e.g. minimal number of dimensions or end-members) and reproducibility on the other hand (Weltje, 1997; Prins & Weltje, 1999), the three-end-member model represents a reasonable solution (Fig. 5c). The grain-size distributions of the three end-members are illustrated in Fig. 5d. The coarser end-members (EM 1 and EM 2) have a well-sorted distribution with a clearly defined mode, whereas the fine-grained end-member (EM 3) has a poorly sorted grain-size distribution with a moderately defined mode ranging from 3 to 5 μm. EM 1 has a modal grain size of ≈43 μm and EM 2 of ≈24 μm. In Fig. 6, the relative contribution of the end-members is mapped across the investigation area. This mapping indicates that the coarsest end-member, EM 1, is only significantly present in samples from the region off

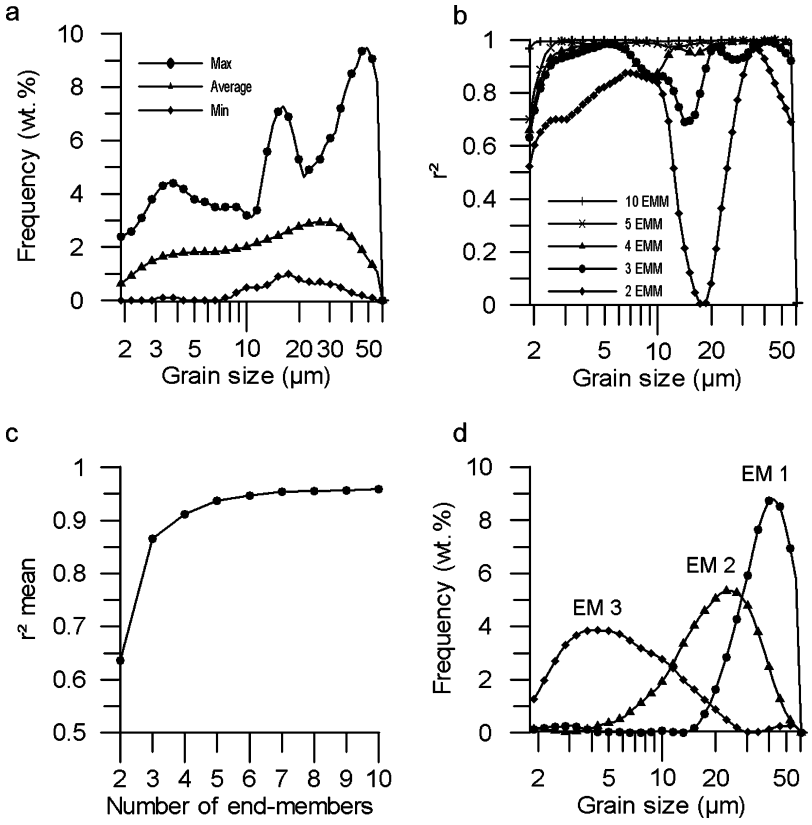

Fig. 5. End-member modelling results of the measured grain-size distributions of the seabed sediments. (a) Summary statistics of input data ($n = 78$); maximum, average and minimum frequency record in each size class. (b) Coefficients of determination (r^2) for each size class of different end-member solutions (2–10 end-members). (c) Mean coefficient of determination (r^2_{mean}) for each end-member model. (d) Modelled end-members of the carbonate-free silt fraction of the seabed sediments of NW Africa.

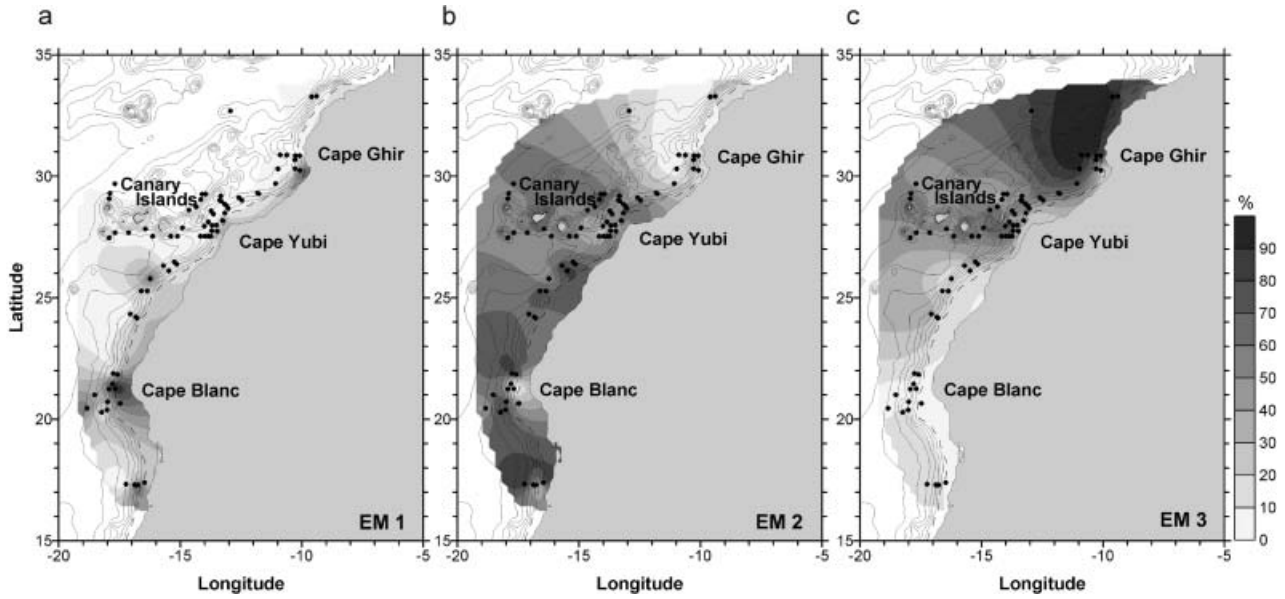

Fig. 6. Spatial variation of modelled end-member contributions of the carbonate-free silt fraction offshore north-west Africa. Seabed sample locations indicated by black dots. Isopleths were calculated using the gridding method of kriging. (a) Contour map of the coarsest end-member, EM 1, reflecting coarse-grained aeolian dust. (b) Spatial distribution of EM 2, fine-grained aeolian dust. (c) Contour map of EM 3 representing fluvially discharged mud.

Cape Blanc between 20°N and about 23°N (Fig. 6a), whereas particle distributions with a modal grain size of about 24 µm (EM 2) are represented along the west African continent and around the Canary Islands (Fig. 6b). Fine-grained particles, which are represented by EM 3, are

confined to the area off Cape Ghir, where the end-member EM 3 builds up to 90% of the relative contribution (Fig. 6c).

DISTRIBUTION OF AEOLIAN AND FLUVIAL SEDIMENTS ALONG THE NORTH-WEST AFRICAN COAST

Natural marine sediments are mainly mixtures of biogenic and terrigenous components. However, the terrigenous fraction itself is a composite and can be assembled by various sources and different transport processes. Thus, the application of the end-member model of Weltje (1994, 1997) is a powerful approach to 'unmix' terrigenous matter into subpopulations that can subsequently be interpreted in terms of origin and/or transport pathways. Moreover, the application of the end-member algorithm to seabed sediments was used to interpret the distribution of the end-members in terms of interaction during transport, deposition and redistribution of the terrigenous particles (i.e. sorting by bottom currents or current focusing revealed by depositional bedforms; Frenz *et al.*, 2003). However, in this study, no reworking of sediments was observed and, therefore, the end-members are interpreted in terms of transport mechanisms only.

The grain size of the aeolian particles in deep-sea sediments depends on the distance to the source and the capacity of the transporting agent. Close to the continent, the sediments are generally coarser grained compared with the distal open ocean. According to deep-sea sediment studies from various areas (Koopmann, 1981; Sarnthein *et al.*, 1981; Sirocko, 1991; Prins & Weltje, 1999; Moreno *et al.*, 2002; Stuut *et al.*, 2002), terrigenous sediments with a modal grain size larger than 6 μm are attributed to aeolian dust fallout, whereas hemipelagic deposition is assumed for particles smaller than 6 μm. Accordingly, EM 1 and EM 2 are interpreted as wind-blown, and EM 3 is inferred as having been supplied from fluvial input. Present-day Saharan dust grain-size distributions along transects off the north-west African coast are used for reference and comparison. The results support the interpretation of EM 1 and EM 2 as aeolian dust. The present-day aerosols, which were collected during February and March 1998, mirror the grain sizes of the supposedly wind-blown end-members. The modal grain sizes of the spring dust plume vary from about 7 μm, characterized as long-distance transported dust, to about 30 μm close to the source area (Fig. 3). In their investigations off NW Africa, Koopmann (1979, 1981) and Sarnthein *et al.* (1981) related the carbonate-free fraction larger than 6 μm in diameter to aeolian sediment supply. Here, the data set is also compared with the supposedly aeolian grain-size data set of Koopmann (1979; modelled by Weltje & Prins, 2003). Weltje & Prins (2003) showed that this data set is best described by five end-members, which are interpreted as downwind-fining aeolian sediments. The five end-members appear to have virtually unimodal grain-size distributions with modal grain sizes between 11 μm for the finest end-member and about 91 μm for the coarsest grain-size subpopulation (Fig. 7a). Care has to be taken in the comparison

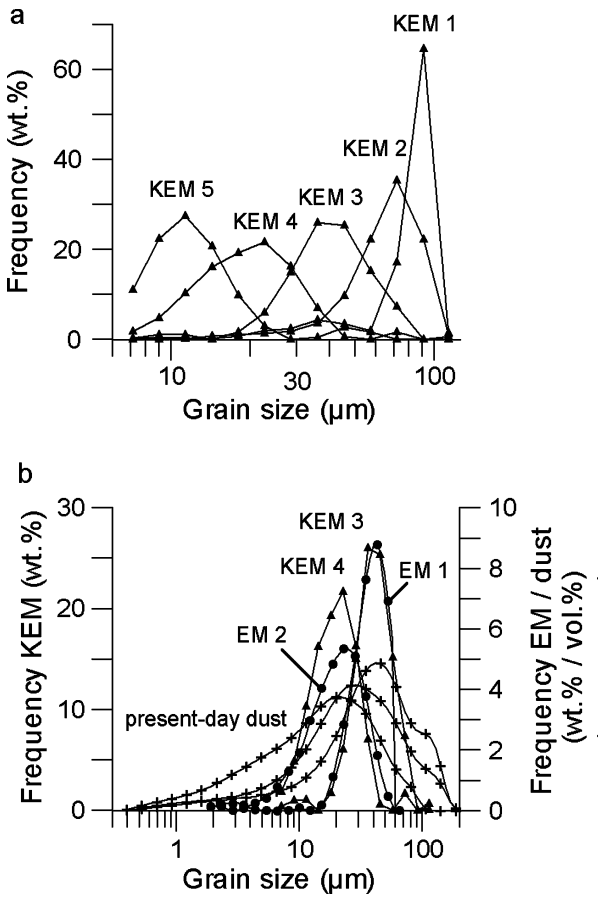

Fig. 7. Modelled end-members are compared with the results of end-member modelling of aeolian sediments offshore NW Africa (Koopmann, 1979) and with grain-size distributions of present-day dust fallout in the investigation area. (a) End-member grain-size distributions modelled by Weltje & Prins (2003). Raw data from Koopmann (1979). (b) Comparison of aeolian end-members EM 1 and EM 2 with end-member grain-size distributions of Koopmann (KEM 3 and KEM 4) and grain-size distributions of present-day aeolian dust samples.

of the different end-members considering the different analytical methods that were used for the various grain-size analyses (Molinaroli *et al.*, 2000). However, the coarsest two (aeolian) end-members of this study (EM 1 and EM 2) compare very well with two of the modelled subpopulations of the Koopmann data set (KEM 3 and KEM 4; KEM = 'Koopmann end-members') with modes of about 23 μm and 36 μm, as well as the present-day dust samples (Fig. 7b). KEM 1 and KEM 2 with modes of about 72 and 91 μm, respectively, are interpreted as exceptionally coarse aeolian sediments (Weltje & Prins, 2003). Although the coarsest present-day dust sample (Fig. 3, dust sample 8) has few particles larger than 100 μm, its mode is around 30 μm. Therefore, KEM 1 and KEM 2 probably have to be attributed to other transport mechanisms, such as turbidity currents, although initially they could have been brought in by wind. Very coarse particles (> 62·50 μm, so-called 'giant' particles) have been shown to be potentially wind-blown (McTainsh *et al.*, 1997; Middleton *et al.*, 2001) and have also been recorded over the Cape Verde Islands (Glaccum & Prospero, 1980) and in the Canary Island region (Coudé-Gaussen, 1989).

The modern dust fallout is well preserved in the examined seabed sediments. The deep-sea sediments offshore NW Africa represent a long-time archive for aeolian transport and dust plumes with variations in wind intensity, source areas and most probably seasonal variability in dust supply. It is observed and widely accepted that dust plays an important role in terrigenous sedimentation off NW Africa (Koopmann, 1981; Sarnthein *et al.*, 1981, 1982; Tetzlaff & Peters, 1986; Moreno *et al.*, 2001), especially offshore of the very arid latitudes of the western Sahara. Fine-grained aeolian dust, which may be transported over long distances or by weakening winds, is deposited widely over the investigated area along the north-west African continental margin. In the south of the area, off Cape Blanc, these relatively fine-grained deposits are overprinted by coarse-grained aeolian dust, while in the northern part, off Cape Ghir, the end-member model outcome suggests fluvial supply to the Atlantic Ocean.

Sarnthein *et al.* (1981) analysed the same Koopmann (1979) data set by Q-mode factor analysis, identifying four grain-size assemblages that account for 99% of the variance. They argued that three of these (factors 1, 2 and 4) were related to aeolian dust, whereas one factor (factor 3) was related to bottom-water transport. The fine fraction (factor 1: 11 μm) was thought to be derived from two sources, representing predominantly aeolian dust but, in some cases, also fluvial discharge, characterized by an excess of fine-grained material < 6 μm, although the latter contribution could not be quantified. The major advantage of the end-member model is that it is able to resolve components in the fine sediment fraction. The spatial distribution of EM 3, which is interpreted as fluvial mud, shows that the fluvial contribution is restricted to the northern part of the north-west African coast (Fig. 6). This interpretation is supported by studies that show that sediment is delivered to the tropical eastern North Atlantic by the Souss River (McMaster & Lachance, 1969; Ercilla *et al.*, 1998; Wynn *et al.*, 2000a). Hence, the dilution of the aeolian fallout in marine sediments through river discharge from southern Morocco and the drainage of the Atlas Mountain hinterland is evident.

Two wind systems are important for this area, the Saharan Air Layer and the NE trade winds. These wind systems deliver aeolian sediments from different source areas (Sahara and Sahel deserts; e.g. Koopmann, 1981; Sarnthein *et al.*, 1981; Tetzlaff & Peters, 1986). Biscaye (1965) investigated the origin of sediments in the eastern Atlantic on the basis of mineralogical analyses and distinguished between Saharan and Sahelian sediments, assuming that the whole terrigenous fraction was of aeolian origin. However, it has been shown here that the terrigenous fraction of sediments in the eastern tropical North Atlantic contains a considerable fluvial fraction as well. Therefore, provenance studies of the different wind systems need to isolate the aeolian fraction only.

CONCLUSIONS

Grain-size distributions of seabed sediments recovered off north-western Africa can be described using an end-member modelling algorithm (Weltje, 1997). The coarsest two end-members are interpreted as 'coarse' and 'fine' aeolian dust and the finest end-member as the result of fluvial supply.

The distributions of the modelled end-members show distinct regional variations. The 'fluvial' end-member is dominant especially in the northern part of the study area, along the Moroccan coast. The different relative proportions of end-members can be related to different transport mechanisms and hinterland climates. North of

29–30°N, rivers drain from the Atlas Mountains, particularly during snow melting and also during rain-intensive seasons. South of 29°N, climatic conditions are more arid and, therefore, the terrigenous supply is restricted to aeolian dust of different grain sizes, varying with the transport distance to the source area.

From the results of the end-member model, the present-day sedimentation pattern off NW Africa can be explained, and input from fine-grained, wind-blown and river-discharged sources can be distinguished. This is important for the reconstruction of palaeoclimate records from grain-size distributions in cores from offshore NW Africa.

ACKNOWLEDGEMENTS

We thank Helge Meggers for providing the seabed samples that were recovered during the CANIGO project (Canary Islands Azores Gibraltar Observations) and also for helpful suggestions. Data presented in this study are available at http://www.pangaea.de. Gert Jan Weltje is thanked for providing the end-member algorithm. The authors gratefully acknowledge the technical assistance of C. Behrens, H. Heilmann and R. Henning in the laboratory. The manuscript was greatly improved by reviews from A. S. Goudie, G. J. Weltje and P. Haughton (editor). This work was funded by the Deutsche Forschungsgemeinschaft as part of the DFG-Research Center 'Ocean Margins' of the University of Bremen. This is contribution RCOM0155.

REFERENCES

Arz, H., Lamy, F., Pätzold, J., Müller, P.J. and **Prins, M.A.** (2003) Mediterranean moisture source for an early-Holocene humid period in the northern Red Sea. *Science*, **300,** 118–122.

Bergametti, G. (1992) Atmospheric cycle of desert dust. In: *Encyclopedia of Earth System Science* (Ed. W.A. Nierenberg), pp. 171–182. Academic Press, San Diego.

Biscaye, P.E. (1965) Mineralogy and sedimentation of recent deep-sea clay in the Atlantic Ocean and adjacent seas and oceans. *Geol. Soc. Am. Bull.*, **76,** 803–832.

Coakley, J.P. and **Syvitski, J.P.M.** (1991) SediGraph technique. In: *Principles, Methods, and Application of Particle Size Analysis* (Ed. J.P.M. Syvitski), pp. 129–142. Cambridge University Press, Cambridge.

Coudé-Gaussen, G. (1989) Local, proximal and distal Saharan dusts: characterization and contribution to the sedimentation. In: *Paleoclimatology and Paleometeorology: Modern and Past Patterns of Atmospheric Transport* (Eds M. Leinen and M. Sarnthein), pp. 339–358. Kluwer Academic Publishers, Dordrecht.

D'Almeida, G.A. (1989) Desert aerosol: characteristics and effects on climate. In: *Palaeoclimatology and Palaeometeorology: Modern and Past Patterns of Global Atmospheric Transport* (Eds M. Leinen and M. Sarnthein), pp. 311–338. Kluwer Academic Publishers, Dordrecht.

D'Almeida, G.A. and **Schütz, L.** (1983) Number, mass, and volume distribution of mineral aerosol and soils of the Sahara. *J. Clim. Appl. Meteorol.*, **22,** 233–243.

Duce, R.A. (1995) Source, distributions, and fluxes of mineral aerosols and their relationship to climates. In: *Dahlem Workshop on Aerosol Forcing of Climate* (Eds R.J. Carlson and J. Heintzenberg), pp. 43–72. Wiley, New York.

Duce, R.A., Liss, P.S., Merrill, J.T., Atlas, E.L. and **Buat-Menard, P.** (1991) The atmospheric input of trace species to the world ocean. *Global Biochem. Cycles*, **5,** 193–259.

Ercilla, G., Alonso, B., Perez-Belzuz, F., Estrada, F., Baraza, J., Farran, M., Canals, M. and **Masson, D.** (1998) Origin, sedimentary processes and depositional evolution of the Agadir turbidite system, central eastern Atlantic. *J. Geol Soc. London*, **155,** 929–939.

Frenz, M., Höppner, R., Stuut, J.-B.W., Wagner, T. and **Henrich, R.** (2003) Surface sediment bulk geochemistry and grain-size composition related to the oceanic circulation along the South American continental margin in the Southwest Atlantic. In: *The South Atlantic in the Late Quaternary: Reconstruction of Material Budget and Current Systems* (Eds S. Mulitza, V. Ratmeyer and G. Wefer), pp. 347–373. Springer Verlag, Berlin.

Glaccum, R.A. and **Prospero, J.M.** (1980) Saharan aerosols over the tropical north Atlantic. *Mineral. Mar. Geol.*, **37,** 295–321.

Goudie, A.S. and **Middleton, N.J.** (2001) Saharan dust storms: nature and consequences. *Earth-Sci. Rev.*, **56,** 179–204.

Harrison, S.P., Kohfeld, K.E., Roelandt, C. and **Claquin, T.** (2001) The role of dust in climate changes today, at the last glacial maximum and in the future. *Earth-Sci. Rev.*, **54,** 43–80.

Hillier, S. (1995) Erosion, sedimentation and sedimentary origin of clays. In: *Origin and Mineralogy of Clays – Clays and the Environment* (Ed. B. Velde), pp. 162–219. Springer Verlag, Berlin.

Kiefert, L. (1994) *Characteristics of Wind Transported Dust in Eastern Australia*. Griffith University, Brisbane, 340 pp.

Kiefert, L., McTainsh, G.H. and **Nickling, W.G.** (1996) Sedimentological characteristics of Saharan and Australian dusts. In: *The Impact of Desert Dust Across the Mediterranean* (Eds S. Guerzoni and R. Chester), pp. 183–190. Kluwer Academic Publishers, Dordrecht.

Koopmann, B. (1979) *Saharastaub in den Sedimenten des subtropisch-tropischen Nordatlantik während der letzten 20.000 Jahre*. PhD Thesis, Christian-Albrechts-Universität zu Kiel, 109 pp.

Koopmann, B. (1981) Sedimentation von Saharastaub im subtropischen Nordatlantik während der letzten 25.000 Jahre. *Meteorol. Forschsergeb.*, **35,** 23–59.

Lonsdale, P. (1982) Sediment drift of the Northeast Atlantic and their relationship to the observed abyssal currents. *Bull. Inst. Géol. Bassin Aquitaine*, **31,** 141–150.

McMaster, R.L. and **Lachance, T.P.** (1969) Northwestern African continental shelf sediments. *Mar. Geol.*, **7,** 57–67.

McTainsh, G.H. (1987) Desert loess in Northern Nigeria. *Z. Geomorphol.*, **31,** 145–165.

McTainsh, G.H. and **Walker, P.H.** (1982) Nature and distribution of Harmattan dust. *Z. Geomorphol.*, **26,** 417–435.

McTainsh, G.H., Nickling, W.G. and **Lynch, A.W.** (1997) Dust deposition and particle size in Mali, West Africa. *CATENA*, **29,** 307–322.

Masson, D.G., Watts, A.B., Gee, M.J.R., Urgeles, R., Mitchell, N.C., Le Bas, T.P. and **Canals, M.** (2002) Slope failures on the flanks of the western Canary Islands. *Earth-Sci. Rev.*, **57,** 1–35.

Middleton, N.J., Goudie, A.S. and **Wells, G.L.** (1986) The frequency and source areas of dust storms. In: *Aeolian Geomorphology* (Ed. W.G. Nickling), pp. 237–260. Allen & Unwin, Boston.

Middleton, N.J., Betzer, P.R. and **Bull., P.A.** (2001) Long-range transport of 'giant' aeolian quartz grains: linkage with discrete sedimentary sources and implications for protective particle transfer. *Mar. Geol.*, **177,** 411–417.

Milliman, J.D. and **Meade, R.H.** (1983) World-wide delivery of river sediment to the oceans. *J. Geol.*. **91,** 1–21.

Mittelstaedt, E. (1991) The ocean boundary along the Northwest African coast: Circulation and oceanographic properties at the sea surface. *Prog. Oceanogr.*, **26,** 307–355.

Molinaroli, E., De Falco, G., Rabitti, S. and **Portaro, R.A.** (2000) Stream-scanning laser system, electric sensing counter and settling grain size analysis: a comparison using reference materials and marine sediments. *Sed. Geol.*, **130,** 269–281.

Moreno, A., Targarona, J., Henderiks, J., Canals, M., Freudenthal, T. and **Meggers, H.** (2001) Orbital forcing of dust supply to the North Canary Basin over the last 250 kyr. *Quatern. Sci. Rev.*, **20,** 1327–1339.

Moreno, A., Cacho, I., Canals, M., Prins, M.A., Sanchez-Goni, M.-F., Grimalt, J.O. and **Weltje, G.J.** (2002) Saharan dust transport and high-latitude glacial climatic variability: the Alboran Sea record. *Quatern. Res.*, **58,** 318–328.

Prins, M.A. and **Weltje, G.J.** (1999) End-member modeling of siliciclastic grain-size distributions: the late Quaternary record of eolian and fluvial sediment supply to the Arabian Sea and its paleoclimatic significance. In: *Numerical Experiments in Stratigraphy; Recent Advances in Stratigraphic and Sedimentologic Computer Simulations* (Eds J.W. Harbaugh, W.L. Watney, E.C. Rankey, R. Slingerland, R.H. Goldstein and E.K. Franseen), *SEPM Spec. Publ.*, **62,** 91–111.

Prins, M.A., Postma, G., Cleveringa, J., Cramp, A. and **Kenyon, N.H.** (2000) Controls on terrigenous sediment supply to the Arabian Sea during the late Quaternary: the Indus Fan. *Mar. Geol.*, **169,** 327–349.

Prins, M.A., Bouwer, L.M., Beets, C.J., Troelstra, S.R., Weltje, G.J., Kruk, R.W., Kuijpers, A. and **Vroon, P.Z.** (2002) Ocean circulation and iceberg discharge in the glacial North Atlantic: inferences from unmixing of sediment size distribution. *Geology*, **30,** 555–558.

Prospero, J.M. and **Carlson, T.N.** (1972) Vertical and areal distribution of Saharan dust over the western equatorial North Atlantic Ocean. *J. Geophys. Res.*, **77,** 5255–5265.

Pye, K. (1987) *Aeolian Dust and Dust Deposits*. Academic Press, San Diego, 334 pp.

Sarnthein, M., Tetzlaff, G., Koopmann, B., Wolter, K. and **Pflaumann, U.** (1981) Glacial and interglacial wind regimes over the eastern subtropical Atlantic and North-West Africa. *Nature*, **293,** 193–296.

Sarnthein, M., Thiede, J., Pflaumann, U., Erlenkeuser, H., Fütterer, D., Koopmann, B., Lange, H. and **Seibold, E.** (1982) Atmospheric and oceanic circulation patterns off northwest Africa during the past 25 million years. In: *Geology of the Northwest African Continental Margin* (Eds U. von Rad, K. Hinz, M. Sarnthein and E. Seibold), pp. 545–604. Springer Verlag, Berlin.

Schulz, H.D. *et al.* (1998) Report and preliminary results of METEOR-Cruise M 41/1, Málaga–Libreville, 13.2.–15.3. 1998. *Ber. Fachber. Geowiss. Univ. Bremen*, **114,** 124 pp.

Seibold, E. and **Fütterer, D.** (1982) Sediment dynamics on the Northwest African continental margin. In: *The Ocean Floor; Bruce Heezen Commemorative Volume* (Eds R.A. Scrutton and M. Talwani), pp. 147–163. John Wiley & Sons, Chichester.

Sirocko, F. (1991) Deep-sea sediments of the Arabic Sea: a paleoclimatic record of the Southwest-Asian monsoon. *Geol. Rundsch.*, **80,** 557–566.

Sirocko, F., Sarnthein, M., Lange, H. and **Erlenkeuser, H.** (1991) Atmospheric summer circulation and coastal upwelling in the Arabian Sea during the Holocene and the last glaciation. *Quatern. Res.*, **36,** 72–93.

Smith, W.H.F. and **Sandwell, D.T.** (1997) Global sea floor topography from satellite altimetry and ship depth soundings. *Science*, **277,** 1956–1962.

Stuut, J.-B.W. (2001) Late Quaternary Southwestern African terrestrial-climate signals in the marine record of Walvis Ridge, SE Atlantic Ocean. PhD Thesis. *Geol. Ultraiect.*, **212,** 115 pp.

Stuut, J.-B.W., Prins, M.A., Schneider, R.R., Weltje, G.J., Jansen, J.H.F. and **Postma, G.** (2002) A 300-kyr record of aridity and wind strength in southwestern Africa: inferences from grain-size distributions of sediments on Walvis Ridge, SE Atlantic. *Mar. Geol.*, **180,** 221–233.

Talbot, R.W., Harriss, R.C., Browell, E.V., Gregory, G.L., Sebacher, D.I. and **Beck, S.M.** (1986) Distribution and geochemistry of aerosols in the tropical North Atlantic troposphere: relationship to Saharan dust. *J. Geophys. Res.*, **91,** 5173–5182.

Tetzlaff, G. and **Peters, M.** (1986) Deep-Sea sediments in the eastern equatorial Atlantic off the African coast and meteorological flow patterns over the Sahel. *Geol. Rundsch.*, **75,** 71–79.

Weaver, P.P.E., Wynn, R.B., Kenyon, N.H. and **Evans, J.** (2000) Continental margin sedimentation, with special reference to the north-east Atlantic margin. *Sedimentology*, **47,** 239–256.

Weltje, G.J. (1994) Provenance and dispersal of sand-sized sediments: reconstruction of dispersal patterns and sources of sand-sized sediments by means of inverse modeling techniques. PhD Thesis. *Geol. Ultraiect.*, **121,** 208 pp.

Weltje, G.J. (1997) End-member modeling of compositional data: numerical-statistical algorithms for solving the explicit mixing problem. *J. Math. Geol.*, **29,** 503–549.

Weltje, G.J. and **Prins, M.A.** (2003) Muddled or mixed? Inferring palaeoclimate from size distributions of deep-sea clastics. *Sed. Geol.*, **162,** 39–62.

Wessel, P. and **Smith, W.H.F.** (1991) Free software helps map and display data. *Eos Trans. Am. Geophys. Union*, **72,** 445–445.

Wynn, R.B., Masson, D.G., Stow, D.A.V. and **Weaver, P.P.E.** (2000a) The Northwest African slope apron: a modern analogue for deep-water systems with complex seafloor topography. *Mar. Petrol. Geol.*, **17,** 253–265.

Wynn, R.B., Masson, D.G., Stow, D.A.V. and **Weaver, P.P.E.** (2000b) Turbidity current sediment waves on the submarine slopes of the western Canary Islands. *Mar. Geol.*, **163,** 185–198.

Manuscript received 15 April 2003; revision accepted 17 June 2004.